SpiroSonic: Monitoring Human Lung Function via Acoustic Sensing on Commodity Smartphones

Xingzhe Song, Boyuan Yang, Ge Yang, Ruirong Chen, Erick Forno, Wei Chen and Wei Gao
University of Pittsburgh

ABSTRACT

Respiratory diseases have been a significant public health challenge. Efficient disease evaluation and monitoring call for daily spirometry tests, as an effective way of pulmonary function testing, out of clinic. This requirement, however, is hard to be satisfied due to the large size and high costs of current spirometry equipments. In this paper, we present SpiroSonic, a new system design that uses commodity smartphones to support complete, accurate yet reliable spirometry tests in regular home settings with various environmental and human factors. SpiroSonic measures the humans' chest wall motion via acoustic sensing and interprets such motion into lung function indices, based on the clinically validated correlation between them. We implemented SpiroSonic as a smartphone app, and verified SpiroSonic's monitoring error over healthy humans as <3%. Clinical studies further show that SpiroSonic reaches 5%-10% monitoring error among 83 pediatric patients. Given that the error of in-clinic spirometry is usually around 5%, SpiroSonic can be reliably used for disease tracking and evaluation out of clinic.

CCS CONCEPTS

• **Human-centered computing** → **Ubiquitous and mobile computing**.

KEYWORDS

Mobile Health, Lung Function, Respiratory Diseases, Acoustic Sensing.

1 INTRODUCTION

Respiratory diseases, such as asthma, chronic pulmonary disease (COPD) and acute respiratory distress syndrome (ARDS), constitute a significant public health challenge [4]. Over 330 million people worldwide have asthma, including 8.4% of children and 7.7%

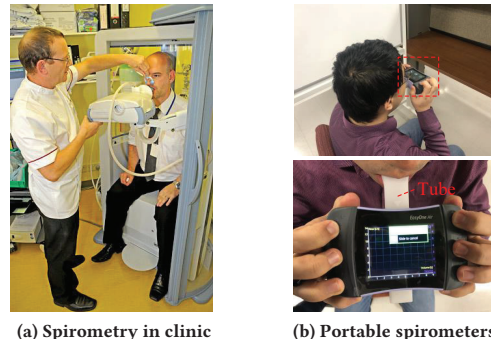(a) Spirometry in clinic (b) Portable spirometers
Figure 1: Current spirometry tests

of adults [21]. These diseases are characterized as various types of airway obstruction. *Spirometry*, as the most commonly used pulmonary function testing (PFT), assesses such obstruction by measuring the volume and velocity of breathing airflow [69], and is crucial in disease evaluation and monitoring [47]. It is also used to judge shortness of breath and airway inflammation, both of which are important symptoms of the coronavirus disease (COVID-19).

Ideally, spirometry should be daily conducted out of clinic, to timely detect and avoid frequent disease exacerbations that cause emergency department visits or hospitalizations [7, 34]. However, current spirometers in clinic, as shown in Figure 1(a), are too bulky for daily home use. Recent efforts, as shown in Figure 1(b), reduce the size of spirometers but their costs (>$2,000) are still too high for home use [1]. Low-cost spirometers priced at <$100 [48, 64] are mostly inaccurate and could produce >20% error [28, 42].

To reduce the cost of portable spirometers without impairing the PFT accuracy, researchers developed wearable sensing systems [13, 25], but required attaching extra hardware to human bodies. Wireless signals were used to analyze humans' breathing patterns from remote, but have low resolution and can only measure the breathing rates [31, 44, 75] and volume [55]. Modern smartphones have been used to derive humans' breathing patterns from smartphones' IMU data [2, 5, 43] or video captures [65]. However, the accuracy of these methods is too low for precise evaluation of lung function. Some recent techniques use smartphones to calculate humans' lung function indices from their audible breathing sounds [23, 39], but require absolutely quiet surroundings and are highly sensitive to ambient noise and human activities in home settings.

In this paper, we present *SpiroSonic*, a novel system design that uses commodity smartphones to support complete, accurate yet reliable spirometry tests out of clinic, with various environmental and human factors. As shown in Figure 2, our design builds on the close correlation between lung function and chest wall motion of humans, which has been widely validated in clinical practice [22, 36, 61, 63]. SpiroSonic measures chest wall motion as an externally observable biomarker, and interprets such motion

Xingzhe Song, Boyuan Yang, Ge Yang, Ruirong Chen, Erick Forno, Wei Chen and Wei Gao

	Physical Contact	Additional Hardware	Accuracy	Cost	Environment Adaptability	Clinical Validation
Wearable sensors [13, 25]	Yes	Yes	Medium	Medium	Medium	Limited
IMU sensor [2, 5, 43]	Yes	No	Low	None	Medium	Limited
Infrared/Depth cameras [40, 74]	No	Yes	High	Very High	Low	None
RF systems [31, 44, 55, 75]	No	Yes	Medium	High	Very Low	None
Smartphone cameras [65]	No	No	Low	None	Very Low	None
Audible sound analysis [23, 39]	No	No	Low	None	Very Low	Limited
Acoustic sensing [51, 52, 72]	No	No	Medium	None	Medium	Extensive
SpiroSonic	**No**	**No**	**High**	**None**	**High**	**Extensive**

Table 1: Comparison of technologies measuring human lung function out of clinic
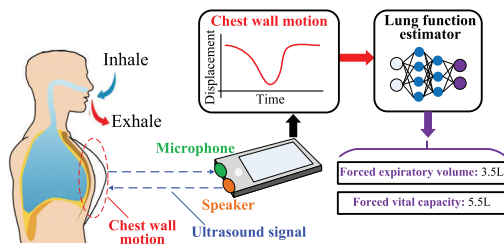

Figure 2: SpiroSonic measures chest wall motion, and interprets such motion into lung function indices.

into lung function indices. To measure such motion, SpiroSonic transmits ultrasound signal with the smartphone's speaker, and analyzes the signal being reflected by the patient's chest wall and received by the smartphone's microphone. In this way, SpiroSonic is 100% contactless and non-intrusive. Some existing work similarly used smartphone's transmitted acoustic signals to measure humans' chest motions [51, 52, 72], but interpreted such motions only into humans' respiration rates or breathing events (e.g., apnea).

To ensure accurate spirometry tests, SpiroSonic's error of measuring chest wall motion should be at most few millimeters. Current acoustic sensing systems achieve such accuracy using a smartphone that is always stationary, when monitoring humans' breath in sleep [15, 27, 52] or tracking small targets' motions (e.g., human fingers) [45, 53, 73, 77]. In contrast, SpiroSonic aims to enable daily spirometry tests anytime and anywhere at home, and we hence assume that users always hand-hold the smartphone when using SpiroSonic, in the same way as they are using commodity portable spirometers. However, when being hand-held, the smartphone's received ultrasound signal could be easily affected by its random motions. To identify the impact of these motions, we convert the received signal to I/Q traces on the complex plane[1], so as to quantify such impact as the geometric distortions of I/Q trace. Then, we adaptively remove such impact by correcting these distortions and calibrating the received signal as if it is produced with a stationary smartphone.

The major challenge of interpreting chest wall motion into lung function indices, on the other hand, is the heterogeneous human factors that may impair the data quality in spirometry tests. For example, patients may fail to follow the spirometry protocol [49], when using SpiroSonic without guidance from clinicians. To eliminate the impact of these human factors, SpiroSonic avoids estimating lung function indices directly from chest wall motion. Instead,

we extract specific features from the chest wall motion, and use these features as the input to a neural network regression model. In particular, these motion features are extracted only from the exhalation stage of spirometry, and we will apply multiple criteria to ensure that such exhalation stage can be appropriately identified.

To our best knowledge, SpiroSonic is the first spirometry system using commodity smartphones in regular home settings. It provides a convenient yet cost-free tool for continuous tracking and evaluation of pulmonary diseases, which are crucial to patients' wellbeing. It also contributes to early-stage diagnosis of COVID-19 out of clinic, and helps reduce the burden of public healthcare system in pandemic. The key characteristics of SpiroSonic are as follows:

- SpiroSonic is *accurate*. Its error of measuring chest wall motion is constrained within 4mm. When being evaluated among healthy humans, its error of lung function monitoring is always lower than 3%.
- SpiroSonic is *adaptive*. It can precisely remove the impact from various environmental and human factors, and allows flexible variations of smartphone's position (up to 20cm) and orientation (up to 30° tilting) during spirometry tests without impairing the accuracy. It also well adapts to humans' body conditions, as well as different types of clothes being worn.
- SpiroSonic is *lightweight*. It is contactless and does not require any extra hardware. It consumes <15% of smartphone's battery life with 1-hour usage.
- SpiroSonic is *easy to use*. It is implemented as an Android app, and its spirometry tests are fully automated and require the minimum involvement from users.

By collaborating with clinical pulmonologists and biostatisticians, we conducted a clinical study in the Children's Hospital of Pittsburgh of 4 months, over 83 pediatric patients that cover different ages, genders, body conditions and diseases. With the IRB approval, all studies were done in clinical rooms when patients visited the hospital for spirometry tests, and 281 data records from tests are collected. Results of our clinical study are as follows:

- SpiroSonic's error of lung function monitoring is between 5% and 10% for most patients. Since the error of in-clinic spirometry is around 5% [16, 37], results from SpiroSonic could be reliably used as clinical evidence.
- We statistically demonstrate that patients' chest wall motion is strongly correlated to their lung function indices, and some of such correlations are linear.
- SpiroSonic achieves high monitoring accuracy over different patient subgroups, divided by age, gender and disease. It is hence widely applicable to the large population of patients.

---

[1]I/Q trace is a 2D representation of the received signal after down conversion, and the signal's real (I) and imaginary (Q) components are exhibited on the complex plane.

2 BACKGROUND & MOTIVATION

We first introduce the clinical background of spirometry, and explain the correlation between lung function and chest wall motion that motivates our design of SpiroSonic.

2.1 Spirometry and Lung Function Indices

Spirometry measures how fast and how much air the patient can breathe out. Before a test starts, the patient exhales all air from the lung. Then, as shown in Figure 3(a), a spirometry test consists of two stages[2]: the patient first takes a full inhalation and then exhales as hard as possible, until no more air can be breathed out [49].

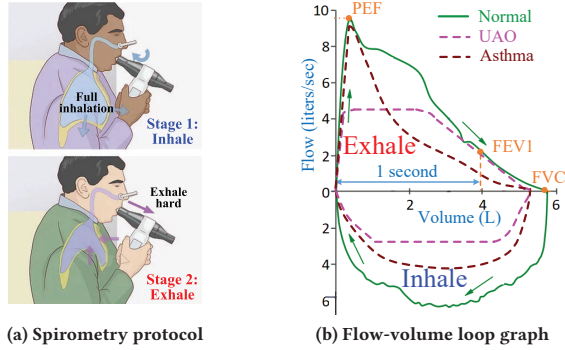**(a) Spirometry protocol**   **(b) Flow-volume loop graph**

Figure 3: Spirometry to evaluate lung function

As shown in Figure 3(b), measurements from spirometry are represented by a flow-volume loop graph that depicts the correlation between the volume and velocity of airflow, and the graphs of patients with pulmonary diseases are significantly different from those of healthy people. For example, patients with upper airway obstruction (UAO) exhibit apparent plateaus in the graph [9], and asthma patients exhibit "scooped" curves in the exhaling part of the graph [46]. In practice, clinicians usually extract certain features from the graph as lung function indices, for more convenient disease evaluation and monitoring. These indices include:

- **Peak expiratory flow (PEF)** is the maximum airflow velocity in exhalation. The average PEF of healthy males and females is around 10L/sec and 8L/sec, respectively. The PEF of asthma patients is as low as 5L/sec [24, 62].
- **Forced expiratory volume in 1 second (FEV1)** is the exhaled air volume in the first second of exhalation, and indicates the airway's resistance against breath [8]. The average FEV1 for healthy people is 3.75L, but that of COPD patients could be as low as 2L [38].
- **Forced vital capacity (FVC)** is the total air volume exhaled. Decline of FVC indicates disease deterioration, and can reach 2.5L for COPD patients [6, 16]. The average FVC of healthy males and females is 5.25L and 3.75L, respectively [37].
- **FEV1/FVC** is the ratio of FEV1 and FVC. This ratio should be >80% among healthy people, but could be as low as 50-60% among asthma patients [12].

In clinical practice, PEF measurements are highly variable [10, 29], and clinicians mainly use the other three indices to evaluate lung function [11]. To ensure accuracy, a patient usually completes multiple (3-8) spirometry tests [19, 20], and the maximum difference

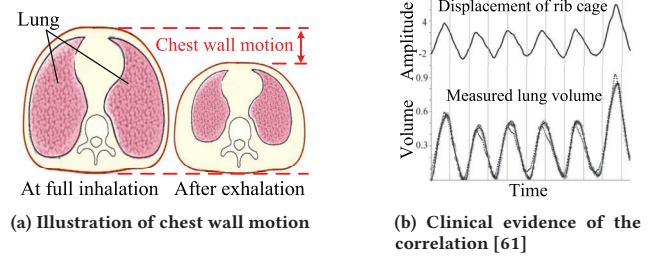[2]https://www.wikihow.com/Take-a-Spirometry-Test

(a) Illustration of chest wall motion   **(b) Clinical evidence of the correlation [61]**

Figure 4: Correlating chest wall motion to lung function

of FEV1 and FVC readings in these tests should be <0.15L [49]. In this way, measurement error of in-clinic spirometry is around 5% [16, 37], which is the baseline to evaluate SpiroSonic's performance.

Since lung function greatly varies over individuals, the raw values of lung function indices are seldomly used in clinic. Instead, clinicians usually categorize patients into subgroups according to their demographics (e.g., age, gender, race, etc.), and then convert the raw values of lung function indices into percentiles (%pred) over healthy people's data in the subgroup, provided by Global Lung Function Initiative (GLI) [60]. Typically, a percentile lower than 70% indicates high risks of pulmonary diseases. SpiroSonic will use such percentiles as indicators to measure human lung function.

### 2.2 Correlation between Lung Function and Chest Wall Motion

Correlation between lung function and chest wall motion has been clinically validated. Such correlation, as shown in Figure 4(a), originates from humans' ribcage expansion and contraction when breathing [17]. These ribcage movements, when measured by a pneumotrace chest band, are consistent with the fluctuation of lung volume as shown in Figure 4(b). Clinical studies also showed that humans' lung volume proportionates to the ribcage motion [61].

Such correlation motivates SpiroSonic to measure the volume of breathing airflow from external, through the displacement of chest wall in spirometry tests. Similarly, the velocity of airflow can be measured from the speed of chest motion. In particular, clinical studies showed that asthma and COPD patients have significantly reduced chest wall motion [36, 63], due to the abnormal changes of chest dimensions and the subsequent lateral ribcage indrawing. For example, patients and healthy people could have 20mm mean difference on the ribcage anteroposterior motion, as well as 10mm mean difference on the upper lateral motion [22].

Such correlation has also been clinically validated to be significant and consistent across different human groups, such as different age groups, males and females with different chest structures and conditions [18], obese people with high BMI [63], etc. Hence, by measuring the patients' chest wall motion, SpiroSonic could potentially serve as a useful tool for pulmonary disease evaluation and tracking out of clinic. Although our clinical study in this paper evaluated SpiroSonic over pediatric patients that are the susceptible population of asthma and COPD, SpiroSonic could also be equally applied to adult patients due to such strong correlation.

3 SYSTEM OVERVIEW

As shown in Figure 5(a), to use SpiroSonic, the patient hand-holds the smartphone and points the phone's bottom speaker and microphone to the chest. Then, the patient follows the spirometry

Xingzhe Song, Boyuan Yang, Ge Yang, Ruirong Chen, Erick Forno, Wei Chen and Wei Gao
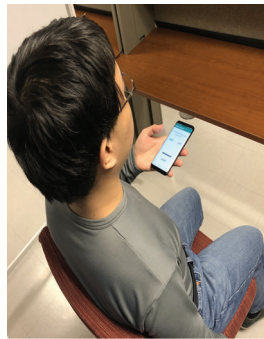
(a) A patient using SpiroSonic
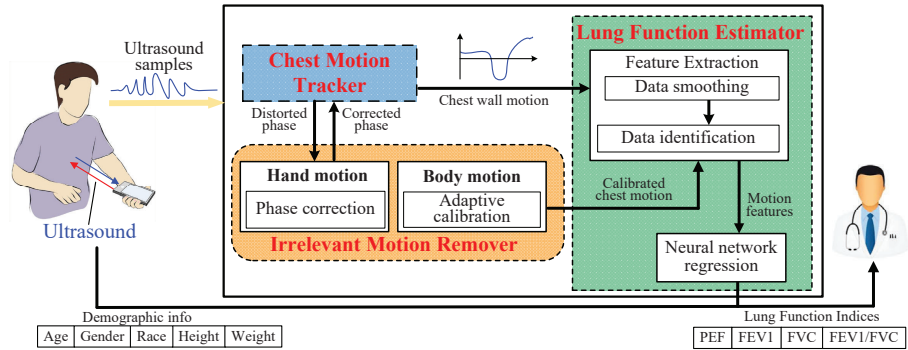
(b) Overall design of SpiroSonic

Figure 5: SpiroSonic system overview

protocol to inhale and exhale. Being similar with in-clinic spirometry, the patient should maintain an upright posture by leaning the back against a chair backrest [49]. In this way, the body trunk remains steady during the spirometry test, and the measured chest wall motion is only caused by inhalation and exhalation.

SpiroSonic tracks the patient's chest wall motion in both inhalation and exhalation stages of spirometry tests. To ensure accuracy, such chest wall motion will be first examined and corrected to remove any impact of irrelevant motions. Afterwards, the corrected chest motion will be used as the input to neural network regression, which computes lung function indices based on the nonlinear correlation between chest wall motion and human lung function. These lung function indices will be converted into %pred values based on the patient's demographic information, and then reported to pulmonary doctors for remote disease evaluation and monitoring.
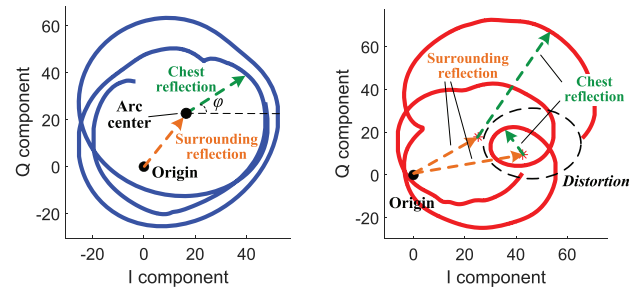
3.1 Chest Motion Tracker

Since humans' chest wall displacement in spirometry is usually lower than 60mm [35], the error of chest motion tracking should be at most 3-4 millimeters, so that the error of lung function estimation could be within 5%. To achieve this accuracy, SpiroSonic measures the phase change between the transmitted and received ultrasound signal. Considering the transmitted signal as $A\cos(2\pi f t)$, the phase of the received signal, after being reflected by the chest wall, is $\varphi(t) = 4\pi f d(t)/c$, where c is sound speed and $d(t)$ is the distance between chest wall and smartphone at time t. When the chest wall moves during a time period $[t_0, t_1]$, its displacement is

$$\Delta d = d(t_1) - d(t_0) = -c/(4\pi f) \cdot (\varphi(t_1) - \varphi(t_0)). \quad (1)$$

When the ultrasound signal's frequency ranges between 17kHz and 24kHz[3], a 2mm displacement causes the signal path length to change by 4mm and corresponds to a phase change between 0.4π and 0.56π, large enough to be detected. Such detectability also allows us to use multiple signals with different frequencies in this range to further improve the tracking accuracy.

3.2 Irrelevant Motion Remover

Since the chest wall's motion is measured as its relative displacement from the smartphone, it could be easily affected by the smartphone's random movements: the patient cannot keep the hand-held

---

[3]17kHz is the lowest inaudible frequency of sound. The acoustic sampling rates of smartphones are usually 48kHz, leading to a maximum ultrasound frequency of 24kHz.

(a) I/Q trace measured with a stationary smartphone

(b) I/Q trace measured with a hand-held smartphone

Figure 6: The impact of irrelevant hand motions on chest motion tracking

smartphone to be 100% stationary, and his/her body may unconsciously lean forward or backward when exhaling hard. To remove such irrelevant movements from the measured chest wall motion, an intuitive method is to measure the smartphone's movements using its built-in accelerometers. This approach, however, is inaccurate due to the error accumulation, when converting accelerometer readings into displacement via double integration [76].
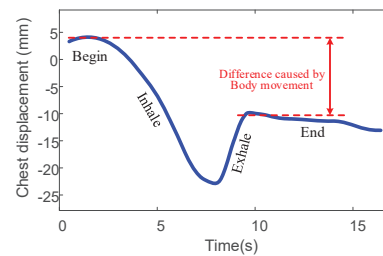

Figure 7: Chest wall motion with body movements

Instead, SpiroSonic investigates the abnormal characteristics from the measured chest wall motion itself. As shown in Figure 6(a), if the smartphone is stationary, I/Q trace of the received signal should be a regular collection of concentric arcs. Otherwise, such I/Q trace produced from a hand-held smartphone with random movements will be arbitrarily distorted. The reason, as shown in Figure 6(b), is that the received signal always contains reflections from both the chest wall and surrounding objects. When the smartphone is hand-held and randomly moving, the surrounding reflection varies and distorts the cumulatively received signal. Details of correcting such distortion will be described in Section 4.1.
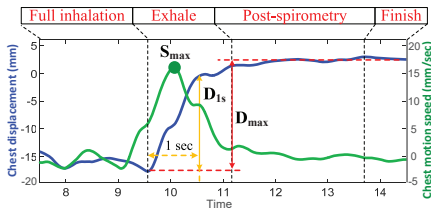
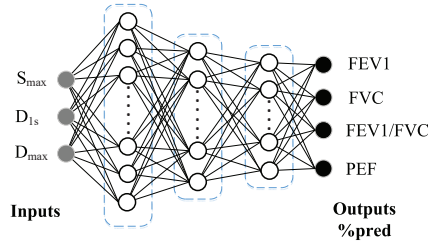Figure 8: Estimating lung function from chest motion
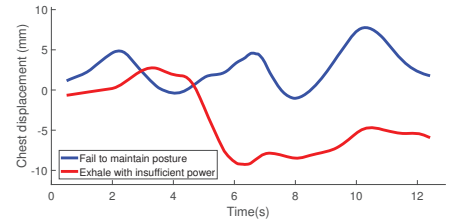

Figure 9: SpiroSonic's neural network

Figure 10: Chest motion from low-quality spirometry tests

Similarly, according to the spirometry protocol in Section 2.1, the patient's chest wall should be at the same position before and after a spirometry test, if the patient's body does not move during the test. The impact of body movements on the measured chest wall motion, as shown in Figure 7, can hence be identified as the difference of chest wall position before and after a spirometry test. Details about removing such body movements are in Section 4.2.

3.3 Lung Function Estimator

As shown in Figure 8, SpiroSonic uses the following features of chest wall motion during the exhalation stage in spirometry to estimate lung function indices:

- The maximum speed of chest wall motion (S_{max}), which corresponds to PEF.
- The chest wall displacement in the first second of exhalation (D_{1s}), which corresponds to FEV1.
- The maximum chest wall displacement (D_{max}), which corresponds to FVC.

SpiroSonic quantifies such correlation with a neural network regression model, which is built with data from clinical studies. Since such clinical data from patients is usually low in volume and could hence result in overfitting when training the model [14], we choose to use a Bayesian regularized neural network, which has good capability of generalization that avoids overfitting [57, 68]. In the clinical study, patients do spirometry tests using SpiroSonic and clinical-grade spirometers at the same time. As shown in Figure 9, the outcomes from SpiroSonic's motion tracking and spirometers' measurements are then used as the inputs and outputs, respectively, to train the neural network[4]. Afterwards, the trained neural network is loaded to patients' smartphones for out-of-clinic use.

Both the accuracy and overhead of such inference depend on the complexity of neural network. A neural network with more hidden layers and numbers of neurons improves the inference accuracy, but also increases its computation overhead. In SpiroSonic, we empirically use three hidden layers in the neural network, and then balance between these two aspects by tuning the numbers of neurons in each layer. In general, we ensure that the numbers of neurons in different hidden layers decrease as the network becomes deeper, and details of such tuning will be in Section 7.

Another challenge of such lung function estimation is the heterogeneous human factors, which may impair the data quality in spirometry tests and make it difficult to correctly identify the exhalation stage. Ideally, the measured chest wall motion, as shown in Figure 8, should exhibit a sole rapid change of chest displacement

of at least 10-15mm, as a result of hard exhalation. However in practice, patients may not fully follow the spirometry protocol, due to lack of clinician's guidance or weak body conditions. As shown in Figure 10, they may exhale with insufficient power and result in inadequate chest displacement; they may fail to keep the upright posture and produce abnormal chest motions. In these cases, details about identifying the exhalation stage are in Section 5.

4 REMOVING IRRELEVANT MOTIONS

In this section, we remove irrelevant smartphone motions and patient body motions from the measured chest wall motion.

4.1 Correcting Signal Distortions due to Smartphone Motions

As shown in Figure 6, motions of a hand-held smartphone distort the I/Q trace of the received ultrasound signal and result in irregular phase variation. To address such variation, SpiroSonic first divides the I/Q traces into short segments, during each of which the smartphone can be assumed as motionless. Then, it approximates each segment back to the closest circular arc on the complex plane. The phase variation can then be corrected by normalizing the centers of all the arcs back to the origin on the complex plane, making the I/Q trace to a collection of concentric arcs as shown in Figure 6(a).

Segmentation: One intuitive method is to divide the I/Q trace into segments with the equal number of signal samples, but is ineffective when chest motion is measured as phase change: as shown in Figure 11(a), since each sample $[I(t), Q(t)]$ has a phase of $tan^{-1}(Q(t)/I(t))$, smaller chest motion results in many consecutive samples with similar phases, and creates many unwanted tiny segments.

Instead, SpiroSonic segments the I/Q trace based on its specific phase change over time. As shown in Figure 11(b), for every two consecutive samples at time t_1 and t_2, we compute the phase change as $(Q(t_2)-Q(t_1))/(I(t_2)-I(t_1))$, and produce a new segment once the cumulative phase change exceeds a threshold. For example, when this threshold is $\pi/2$, the I/Q trace in Figure 11(b) is divided into 6 segments. In practice, SpiroSonic adaptively adjusts this threshold, to make sure that each segment contains a sufficient number of signal samples for correcting the signal distortions. The segment 2 in Figure 11(b), as an instance, corresponds to fast chest motion and hence a larger threshold of π is being applied.

Random signal noise may be produced by the hardware imperfection of smartphones or surrounding signal sources (e.g., spinning fans), and temporarily fluctuates the signal phase as shown in Figure 11(b). Such phase fluctuation may result in small unwanted segments, but unfortunately cannot be removed by smoothing the

---

[4]Lung function indices measured by spirometers are converted into %pred, as described in Section 2.1, before being used to train the neural network.
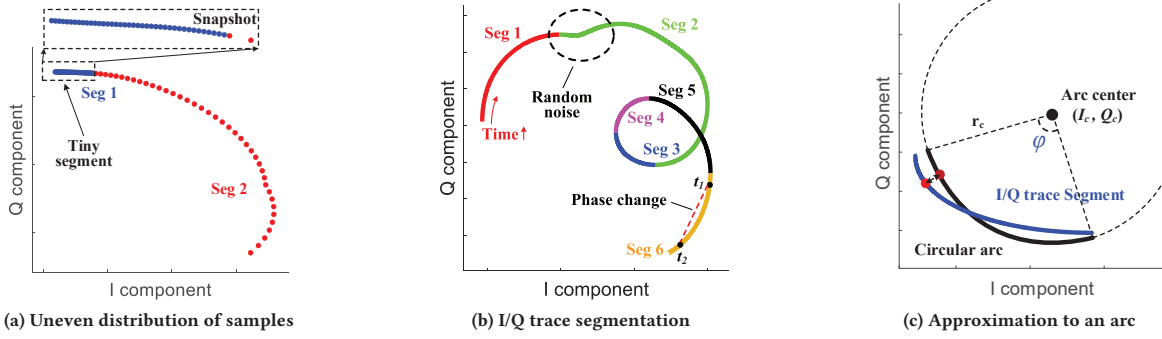
(a) Uneven distribution of samples **(b) I/Q trace segmentation** **(c) Approximation to an arc**

Figure 11: Correcting signal distortions due to smartphone motions
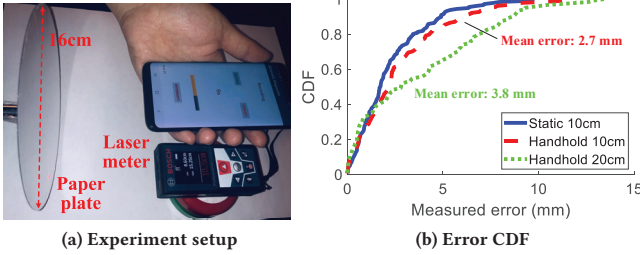

(a) Experiment setup **(b) Error CDF**

Figure 12: Performance of correcting distortions

I/Q trace with a sliding window, due to the uneven distribution of signal samples shown in Figure 11(a). Instead, we avoid such unwanted segments by setting up a threshold on the minimum segment length. This threshold is empirically set as three times of the standard deviation of I/Q samples during full inhalation in spirometry, where the chest wall motion is considered as minimum.

Correction: As shown in Figure 11(c), we approximate each segment to the closet circular arc, indicated by the best linear unbiased estimates (BLUE) of arc center (I_c, Q_c) and radius r_c. This arc[5] is estimated as $[\hat{I}_c, \hat{Q}_c, \hat{\theta}]^T = \left(H^T H\right)^{-1} H^T Y$, where

$$H = \begin{bmatrix} 2I(1) & 2Q(1) & 1 \\ 2I(2) & 2Q(2) & 1 \\ \vdots & \vdots & \vdots \\ 2I(N) & 2Q(N) & 1 \end{bmatrix}, Y = \begin{bmatrix} I(1)^2 + Q(1)^2 \\ I(2)^2 + Q(2)^2 \\ \vdots \\ I(N)^2 + Q(N)^2 \end{bmatrix}, \quad (2)$$

N is the segment's number of samples, and $\hat{\theta} = \hat{r}_c^2 - \hat{I}_c^2 - \hat{Q}_c^2$. Each sample is then mapped to the arc individually.

We evaluate the effectiveness of such correction, as shown in Figure 12(a), by tracking the motion of a round paper plate and using a laser distance meter as the ground truth. Results in Figure 12(b) show that, when the paper plate moves back and forth at different distances, SpiroSonic's motion tracking error approximates to that with a stationary smartphone, and is capped at 3.8mm that meets the requirements for accurate lung function estimation.

4.2 Calibration against Body Motions

Our proposed calibration builds on the fact that the patient's chest wall should be at the same position before and after a spirometry test if there is no extra body motion during the test, because the patient is supposed to have full inhalation and exhalation in spirometry. To

[5]The corresponding circular arc is represented as $(I - I_c)^2 + (Q - Q_c)^2 = r_c^2$.

verify this, we attached a digital accelerometer to the patients' upper body to measure their body motions in spirometry, and results in Figure 13(a) match our expectation. In contrast, with noticeable body motions being indicated by the high accelerometer readings during exhalation, the patients' chest wall position will be largely changed after spirometry tests, as shown in Figure 13(b) and 13(c).

In practice, such body motions could be either unidirectional or bidirectional during exhalation. For unidirectional (i.e., either moving forward or backward) motions, our approach to removing its impact, as described in Algorithm 1, uses the chest wall position before spirometry as the baseline, to proportionally calibrate every signal sample after the exhalation starts. The outcomes, as shown in Figure 13(b) and 13(c), effectively remove the difference of chest wall positions before and after spirometry.

Algorithm 1 Calibration against body movements

Input: $D(t)$: the received ultrasound signal, $t = 1...T$.
   $\Delta D = D_{after} - D_{before}$: difference of chest wall position
Output: $D'(t)$: the calibrated chest wall motion, $t = 1...T$
1: **Initialize** $t_{start} \leftarrow$ exhaling starts, $t_{end} \leftarrow$ exhaling ends;
2: $\Delta d \leftarrow \Delta D / (t_{end} - t_{start})$
3: **for** $t_{start} < t \leq t_{end}$ **do**
4:    $D'(t) \leftarrow D(t) - \Delta D \times \frac{t - t_{start}}{t_{end} - t_{start}}$
5: **for** $t_{end} < t \leq T$ **do**
6:    $D'(t) \leftarrow D(t) - \Delta D$

In some other cases, the patient's body may move both back and forth during exhalation. When such bidirectional body motion is small, SpiroSonic removes this motion through adaptive smoothing: it adapts the smoothing window (W) to the momentary chest motion speed (S) as $W = (1 - |S/S_{\max}|) \cdot f_s$, where $S_{\max}$ is the maximum chest motion speed and f_s is the ultrasound signal's sampling rate. In this way, slower motion leads to a larger window that produces a more smooth motion curve. Rapid motion results in a smaller window to avoid missing details in the motion pattern.

Big bidirectional body motions, on the other hand, indicate that the patient does not follow the spirometry protocol and SpiroSonic will instead judge the corresponding spirometry test as invalid. We will describe details of such judgment in Section 5 and evaluate the effectiveness of such body motion removal in Section 7.

5 IDENTIFYING THE EXHALATION STAGE

The exhalation stage in a spirometry test is indicated by a starting point (p_{start}) and an ending plateau (P_{end}). A valid p_{start} should
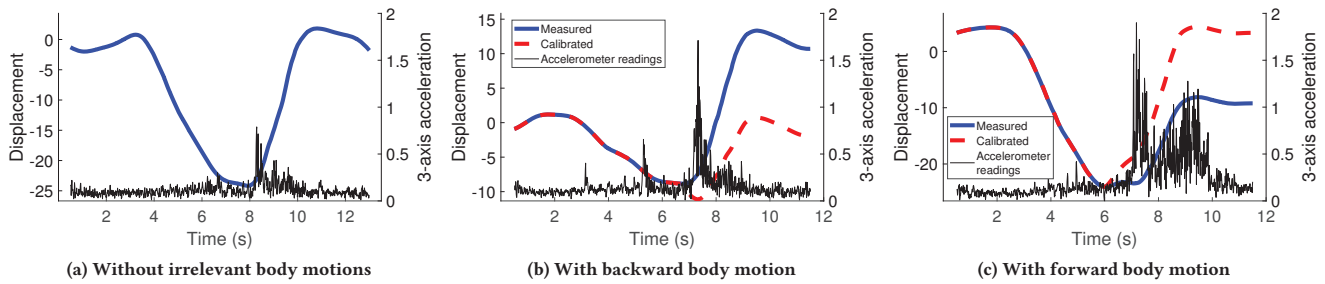
Figure 13: The impact of irrelevant body motions on chest wall motion tracking

be a local minimum on the curve of chest wall displacement, and a valid P_{end} should correspond to a period of sufficiently small chest motion[6]. However in practice, as shown in Figure 14, there may be multiple possibilities of such starts and ending plateaus due to the heterogeneous human factors. We use the following three criteria to decide the best choices of p_{start} and P_{end}:

- p_{start} and P_{end} are always decided in pairs, and the p_{start} always locates before P_{end}.
- The average chest wall displacement within P_{end} should be higher than 90% of the maximum displacement between p_{start} and P_{end}.
- If multiple pairs are available, the pair that corresponds to the maximum chest displacement in exhalation is selected.

Based on such decision, the motion features (S_{max}, D_{1s} and D_{max}) can be calculated as shown in Figure 8. If a valid pair of p_{start} and P_{end} cannot be found, we consider that the patient did not fully follow the spirometry protocol (e.g., the body moves back and forth during exhalation), and data in this spirometry test has low quality. We will exclude such data from lung function estimation.
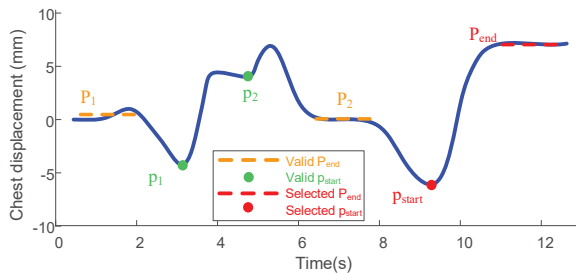

Figure 14: Multiple choices of p_{start} and P_{end}

6   IMPLEMENTATION

As shown in Figure 15, we implemented SpiroSonic as an Android smartphone app that transmits multi-tone ultrasound signals. It uses 12 ultrasound frequencies ranging from 17kHz to 22.5kHz with 0.5kHz interval, which have been proved to have good frequency responses on commodity smartphones [70]. Being similar with previous work [70], we disabled the smartphone's Automatic Gain Control (AGC) to avoid unwanted fluctuations of the received signal amplitude when the ambient noise level varies[7]. The measured

chest wall motion is also adaptively smoothed before any feature extraction, using a flexible sliding window.
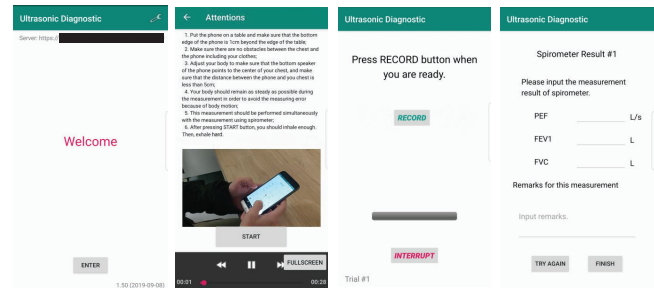

Figure 15: Main screens of SpiroSonic smartphone app

We design the SpiroSonic app following instructions from pulmonary clinicians, to minimize the patients' cognitive and operational barriers when using SpiroSonic out of clinic. Before a spirometry test starts, a tutorial with both texts and video is provided to demonstrate the protocol. A spirometry test using SpiroSonic is: 1) fully automated that no manual inputs (e.g., indicating the start and end of inhalation and exhalation stages) are needed from the patient; 2) fully customizable that the patient can opt to pause or resume the ultrasound recording at any time. We also allow uploading the test results using clinical spirometers, so that this app can also be used in clinical studies (see Section 8).

7   EVALUATION

We evaluate SpiroSonic's accuracy of measuring humans' lung function over five healthy student volunteers with different body conditions[8]. All experiments are conducted in a 10m×10m office with regular furniture and facilities, and student volunteers are instructed to strictly follow the spirometry protocol. Every student volunteer, as shown in Figure 16, conducts 50 spirometry tests using an EasyOne portable spirometer [1], and simultaneously hand-holds a smartphone (Samsung Galaxy S8, OnePlus 7 Pro or XiaoMi Mix 2) running SpiroSonic. The distance between the smartphone and chest wall varies between 5cm to 20cm.

For each student volunteer, we use the other four volunteers' data (spirometer readings and SpiroSonic's measured chest wall motion) to train the neural network regression model. The trained model is used to convert this student volunteer's chest wall motion into lung function indices, which are then compared with the corresponding spirometer results to evaluate the measurement accuracy. Finally, the experiment result is averaged over all the five volunteers.

---

[6] According to the pulmonary clinicians, if the variance of chest wall displacement within 1.5 seconds is less than 15% of the maximum displacement in a test, we consider that 1.5 seconds of chest wall motion as a valid P_{end}.

[7] Since SpiroSonic is designed to receive ultrasound signal within a short range (<20cm), it has good SNR (>40dB) even when disabling the AGC.

[8] Ages: 21-28, Height: 173-188cm, Weight: 55-85kg.

Xingzhe Song, Boyuan Yang, Ge Yang, Ruirong Chen, Erick Forno, Wei Chen and Wei Gao

(a) Small bidirectional body motion **(b) Large bidirectional body motion**
Figure 18: Effectiveness of removing body motions

of both signal segmentation and correction are shorter than 0.3% of the signal segment, ensuring timely system response. Further, calibration against body motions is only applied once to the measured chest wall motion, and it takes 42.8ms on average to execute Algorithm 1 over a 15-second recording of chest wall motion.

7.1 Effectiveness of Irrelevant Motion Removal

Accurate lung function estimation builds on effective removal of the irrelevant smartphone and human body motions. To evaluate such effectiveness, we examine SpiroSonic's error of measuring chest wall motion with three types of typical hand-held smartphone motions shown in Figure 17(a), by comparing SpiroSonic's measured chest wall displacement with the ground truth measured by the laser meter shown in Figure 12(a). The smartphone is hand-held at 10cm away from the chest. Results in Figure 17(b) show that these smartphone motions lead to a maximum measurement error of 3.9mm, which is consistent with that in Figure 12(b).
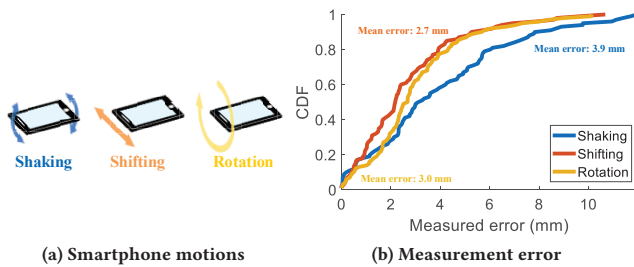

(a) Smartphone motions **(b) Measurement error**
Figure 17: Effectiveness of removing smartphone motions

Further, we discovered that 91.6% of the measured chest motions contain either unidirectional or small bidirectional body motions during exhalation. The small bidirectional body motions, as shown in Figure 18(a), can be sufficiently removed by adaptive smoothing in SpiroSonic, as long as the amplitude of bidirectional portion (*a*) is smaller than 35% of the entire amplitude of body motion (*b*). The large bidirectional body motions, as shown in Figure 18(b), can be 100% identified as invalid by the proposed technique in Section 5.

Segmentation threshold	Segment duration (ms)	Segmentation latency (ms)	Correction latency (ms)
$\pi/2$	186.98	0.32	0.49
π	226.08	0.36	0.54
$3\pi/2$	270.51	0.37	0.67

Table 2: Computational complexity of motion removal

We also evaluated the computational complexity of these motion removal techniques, when being executed on a Samsung Galaxy S8 smartphone. First, algorithms for hand motion removal are evaluated with different phase thresholds for segmentation. As discussed in Section 4.1, the larger this threshold is, the longer each segment will be and the higher computation overhead will be produced. However, as shown in Table 2, in all cases, the computing latencies
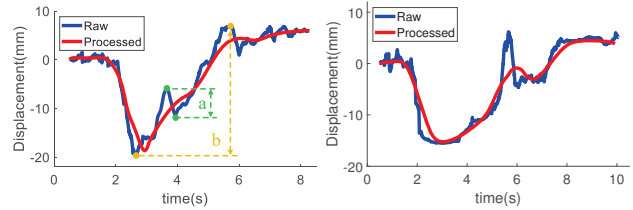
7.2 Measurement Accuracy

As discussed in Section 3.3, accuracy of SpiroSonic's lung function estimation depends on the complexity of neural network being used. Such complexity also decides the computation overhead of online inference. We investigate these two aspects with different numbers of neurons in each hidden layer of the neural network. In all experiments, we use a Samsung Galaxy S8 phone at 5cm from the chest for measurement. Results in Figure 19 show that errors of estimating all the lung function indices can be effectively constrained below 2.5%, when the average number of neurons in each layer is higher than 8. Otherwise, when this average number is reduced to 6, the estimation error could approach to 3%. On the other hand, the computing time of neural network inference is proportional to the neural network complexity. Based on these results, we set the numbers of neurons in the three hidden layers as [12,10,8], for all evaluations in this paper.
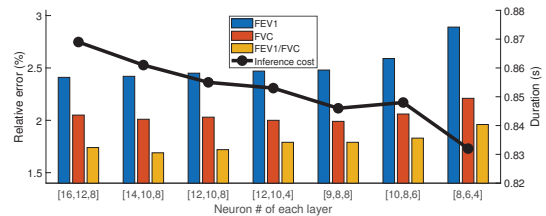

Figure 19: Tradeoff between accuracy and overhead of neural network inference in SpiroSonic

Based on this setup, we first examine SpiroSonic's measurement accuracy with the raw chest wall motion, which is directly produced by the motion tracker in Section 3.1 with lower accuracy. As shown in Figure 20, the average errors of estimating FEV1, FVC and FEV1/FVC are 7.3%, 6.0% and 4.6%, respectively. In particular, it is generally harder to precisely estimate FEV1, because the uncertainty in human behaviors usually makes it difficult to precisely locate p_{start}. On the other hand, when the proposed techniques in Section 4 are used to remove irrelevant hand and body motions, SpiroSonic can reduce the measurement errors to 2.5% and hence reach the same level of accuracy as that of in-clinic spirometry.

7.3 Impact of Different Smartphone Positions

When the distance between the smartphone and chest wall increases, the ultrasound signal strength attenuates and more multipath interferences are also involved. As shown in Figure 21(a),
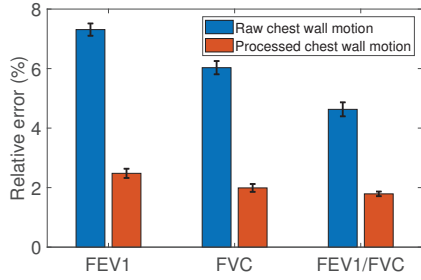
Figure 20: Lung function estimation error of SpiroSonic

when such distance increases from 5cm to 20cm, SpiroSonic's error when measuring FEV1 slightly increases to 2.5%, because the extra signal distortions make it harder to correctly identify the start of exhalation stage. At the same time, SpiroSonic is able to retain the accuracy of measuring FVC and FEV1/FVC with negligible difference over these distances. These results enhance the usability of SpiroSonic out of clinic, as users do not need to intentionally fix the distance between the smartphone and chest wall.
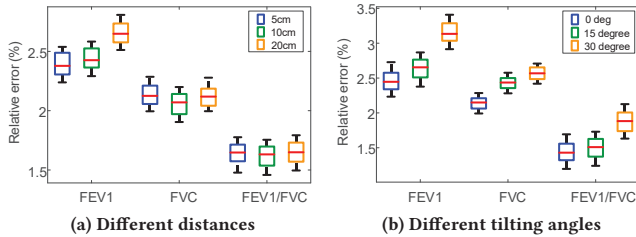

(a) Different distances   **(b) Different tilting angles**

Figure 21: Measurement accuracy with different smartphone positions

When being hand-held, the smartphone may be randomly tilted from horizontal, especially during the exhalation stage. Such tilted positions change the reflection path of ultrasound signal and hence may also affect the measurement of lung function indices. To examine such impact, we keep the measurement distance to be 5cm and tilt the smartphone up and down with different degrees. Experiment results in Figure 21(b) show that when the smartphone is tilted up or down by 15 degrees, the increase of measurement error could be effectively restrained within 0.2%. Even when the smartphone is tilted to 30 degrees, such error will not exceed 3.5%.

7.4 Impact of Smartphone Models

According to [70], different smartphone models may exhibit heterogeneous frequency responses and amplifier gains on the received ultrasound signal, resulting in extra signal distortions. To investigate such impact of different phone models, we run the same SpiroSonic app over three smartphone models running Android 10. Experiment results in Figure 22(a) show that the variance of measurement error is within 0.5%, and the errors over all phone models are always lower than 3%. These results show that the neural network model being used by SpiroSonic can effectively eliminate the impact of irregular amplitudes of ultrasound signal, and demonstrate the general usability of SpiroSonic in practice.

7.5 Impact of the Surroundings

To investigate the reliability of SpiroSonic in practical out-of-clinic environments with noisy surroundings, we tested SpiroSonic with different ambient noise conditions. As shown in Figure 22(b), it
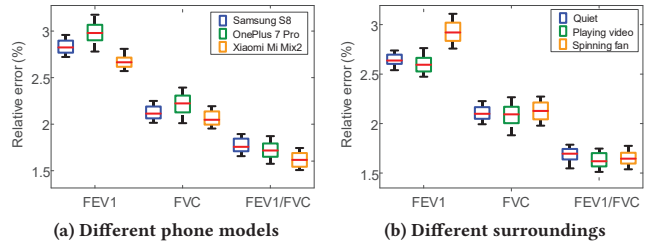

(a) Different phone models   **(b) Different surroundings**

Figure 22: Impact of different smartphone models and surroundings

exhibits great resistance again ambient vocal noise from video playback, which results in negligible error increase. Other sound sources, such as a spinning fan, could increase the measurement error by 0.5% due to the ultrasound components being produced. However, SpiroSonic is still able to restrain such error with 3%.

(a) Different types of clothes being worn

(b) Measurement error with different clothes
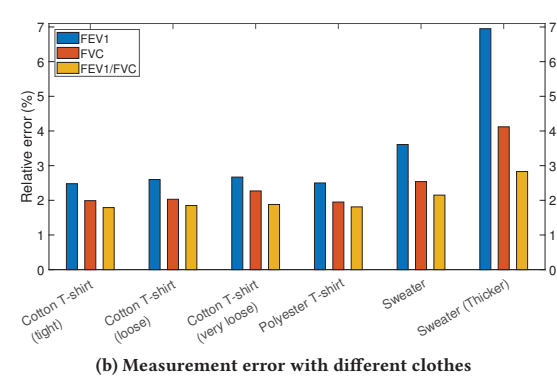
Figure 23: Impact of wearing different clothes

7.6 Impact of Different Clothes

The ultrasound signal, when penetrating through clothes, may create extra reflections that affect the chest motion tracking. To investigate such impact of clothes, we instruct the volunteers to wear clothes of different tightness, thickness and texture, as shown in Figure 23(a). Experiment results in Figure 23(b) show that SpiroSonic provides reliable lung function estimation with most types of clothes, and could effectively restrain the variance across different clothes within 0.5%. The only exception is when the patient wears a thick sweater, which results in significant signal attenuation and raises the measurement error to 7%. However, this thick sweater is for outdoor wear and we do not expect any patient to wear it indoors.

Xingzhe Song, Boyuan Yang, Ge Yang, Ruirong Chen, Erick Forno, Wei Chen and Wei Gao

Figure 24: Power consumption of SpiroSonic

7.7 Power Efficiency

SpiroSonic continuously transmits and records ultrasound signals with smartphone. To evaluate the smartphone's power consumption when using SpiroSonic, we shut down the smartphone's wireless connectivity and all the unnecessar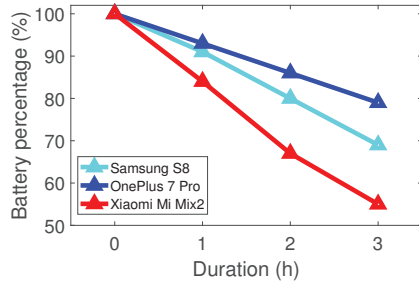y background services. The smartphone's screen is also kept off during the test. Experiment results in Figure 24 show that SpiroSonic is power-efficient and consumes at most 15% of battery life after 1-hour usage. Since each spirometry test only takes less than 10 seconds, the power consumption of SpiroSonic is negligible in practice.

8 CLINICAL STUDY

Based on the high measurement accuracy over healthy humans, we further conducted an observational clinical study at the Children's Hospital of Pittsburgh, to investigate the accuracy of SpiroSonic on measuring the lung function of pulmonary disease patients, particularly, pediatric patients with limited capabilities of cognition and cooperation. With the IRB approval[9], we recruited 83 pediatric patients in 4 months, and requested each patient to use SpiroSonic when they visited the hospital for in-clinic spirometry. The testing setup[10] is shown in Figure 25, and SpiroSonic's accuracy is evaluated with patient data in the similar way as in Section 7.

Figure 25: Test setup in clinical study

As shown in Table 3, the recruited patients cover a wide variety of different ages, genders, races, body conditions and diseases. A total number of 281 spirometry tests are measured, and 185 of them are considered as valid based on the technique in Section 5.

8.1 Statistical Analysis

We statistically analyzed the correlation between patients' chest wall motion and lung function indices. Table 4 shows the Pearson correlation between chest wall motion features (S_{max}, D_{1s},

[9]University of Pittsburgh IRB approval No. STUDY19030114.
[10]Due to the hospital's regulatory requirements to ensure clinical compliance and the pediatric patients' body safety in the clinical room, the smartphone is fixed by a holder in front of chest rather than being hand-held.

Category	Characteristics	Number
Demographics	Tests per patient	2.2 ± 1.4
	Age (years)	11.5 ± 2.6
	Female (%)	40 (48.2)
Body conditions	Height (cm)	148.7 ± 15.3
	Weight (kg)	46.3 ± 19.9
	BMI (kg/m^2)	20.2 ± 5.3
	Underweight (%)	19 (22.9)
	Overweight (%)	14 (16.9)
	Obese (%)	1 (1.2)
Pulmonary diseases	Asthma (%)	62 (74.7)
	Cystic fibrosis (%)	21 (25.3)

Table 3: Patients' Information

D_{max}) and lung function indices. It demonstrates that FEV1, FVC and FEV1/FVC have strong correlations ($P < 0.01$) with chest motion features, clinically validating the usefulness of SpiroSonic. The correlation with PEF is weaker due to high variability of PEF measurements and uncertainty of pediatric patients' body movements.

Corr. Coeff. (P-value)	D_{1s}	D_{max}	S_{max}
FEV1	0.33 ($3.9e^{-6}$)	0.25 ($7.6e^{-4}$)	0.31 ($1.3e^{-5}$)
FVC	0.3 ($3.1e^{-5}$)	0.22 ($2.3e^{-3}$)	0.3 ($3.6e^{-5}$)
FEV1/FVC	0.17 ($1.8e^{-2}$)	0.15 ($4.2e^{-2}$)	0.16 ($3.1e^{-2}$)
PEF	0.12 ($9e^{-2}$)	-0.013 ($8.6e^{-1}$)	0.059 ($4.3e^{-1}$)

Table 4: Pearson correlation between chest wall motion features and lung function indices (%pred).

Furthermore, we individually investigated the correlation between each lung function index and chest motion features, by using generalized linear regression. Results in Table 5 show that all three motion features are linearly correlated with FEV1 and FVC ($P < 0.01$). For example, each millimeter increment of D_{1s} is significantly associated with 1.26 increase of %pred FEV1 and 1.00 increase of %pred FVC. Such correlation with PEF, however, is weaker.

β-Coeff. (P-value)	FEV1	FVC	FEV1/FVC	PEF
S_{max}	0.74	0.62	0.21	0.01
	(< 0.01)	(< 0.01)	(0.03)	(0.16)
D_{1s}	1.26	1.00	0.37	0.04
	(< 0.01)	(< 0.01)	(0.02)	(0.02)
D_{max}	0.54	0.43	0.19	0.01
	(< 0.01)	(< 0.01)	(0.04)	(0.42)

Table 5: Linear correlation between chest motion features and lung function indices (%pred)

Overweighted and obese patients are more likely to exhibit abnormal chest wall motion. To investigate such impact on SpiroSonic, we calculated the above statistical correlation over these patients. Results in Table 6 show that statistical correlations are generally weaker over these patients due to their heterogeneous external characteristics of the chest wall, and strong correlations are only found between chest motion features and FVC.

β-Coeff. (*P*-value)	FEV1	FVC	FEV1/FVC	PEF
S_{max}	0.99 (0.06)	1.47 (< 0.01)	-0.31 (0.12)	-0.07 (0.02)
D_{1s}	1.81 (0.02)	2.46 (< 0.01)	-0.41 (0.17)	-0.09 (0.05)
D_{max}	0.44 (0.40)	1.12 (0.03)	-0.50 (< 0.01)	-0.08 (< 0.01)

Table 6: Statistical correlation among overweight patients

8.2 Accuracy of Estimating Lung Function

Built on the statistical correlation shown in Section 8.1, we investigate SpiroSonic's accuracy of lung function monitoring. Such accuracy is evaluated at both levels of individual spirometry tests and patients. Results in Figure 26 show that at test level, SpiroSonic has an error of 15.45% ± 1.82% and 11.46% ± 1.23% when estimating FEV1 and FVC, respectively. The main reason for such errors is that pediatric patients usually have difficulty in fully following the spirometry protocol and exhibit more diversity in chest wall motion. Besides, such estimation accuracy has been greatly improved from current low-cost spirometers (>20% in home use), and the accuracy in estimating FEV1/FVC is further reduced to <10%.
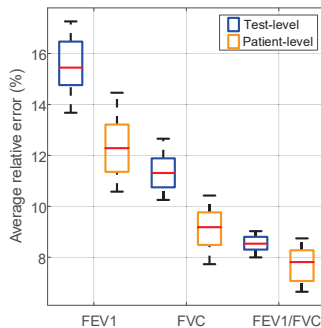

Figure 26: Average errors of estimating lung function indices (all in %pred)

The estimation error at patient level can be reduced to 12.52% ± 1.97%, 9.06% ± 1.39%, and 7.69% ± 1.69% for FEV1, FVC and FEV1/FVC, respectively, by averaging the results from multiple spirometry tests of the same patient. Since a patient's spirometry tests are only valid if the variance of their results is smaller than 10% [19, 49], such patient-level estimation is more commonly used in practice. The accuracy of estimating FEV1/FVC, in particular, approximates to that of in-clinic spirometry (around 5%). SpiroSonic, hence, can be reliably used for disease tracking out of clinic.

We also provide detailed analysis of estimation error for individual patients. As shown in Figure 27, such error exhibits great heterogeneity over different patients. The data quality of three patients (#36, #57 and #80) is extremely low and leads to >60% estimation error. SpiroSonic's estimation error over the rest majority of patients is much lower and ranges between 5% and 10%.

8.3 Estimation Errors over Different Subgroups

In clinical practice, humans' lung function is highly relevant to their age, gender and the specific pulmonary disease they have. Hence, we investigate the accuracy of SpiroSonic' lung function estimation over these different patient subgroups.

Age: We divide patients into three age groups (8-10, 11-13 and 14-17), and numbers of patients in these groups are 34, 26 and 23, respectively. Results in Figure 28(a) show that SpiroSonic's estimation is more accurate over older patients, and the error over age group of 14-17, in particular, has >4% less errors than other groups. The primary reason is that pediatric patients in low ages usually cannot maintain their bodies fully stationary during spirometry tests. In these cases, being different from in-clinic spirometry that measures patients' exhaling airflow through a mouthpiece as shown in Figure 25, SpiroSonic is more sensitive to patients' body motions and produces more errors. This is also exemplified by the ratio of valid spirometry tests in different age groups, which is 70.1% for the Age 14-17 group but only 61.9% for the Age 8-10 group.

In older age groups, estimating FVC is more accurate compared to FEV1 estimation, because older patients have smaller variation of airway caliber with respect to lung size. It is hence easier to estimate their air volumes being exhaled [78].

Gender: Figure 28(b) shows that SpiroSonic achieves higher estimation accuracy over females, and such difference could be up to 3%-4% for estimating FEV1/FVC. One possible reason is that girls' spirometry tests in our clinical study have a higher percentage (69.6%) to be valid, and this percentage is only 62.2% for boys' spirometry tests in our clinical study. Such difference is even more significant in low-age groups. Furthermore, from the clinical perspective, girls usually have wider but shorter airways in their childhood than boys, so that their momentary lung function indices (e.g., FEV1) could have less variation [30]. Further verification of this hypothesis, however, requires larger volumes of patient data and we plan to recruit more patients into clinical study in the future.

Disease: As shown in Figure 28(c), SpiroSonic achieves better accuracy in estimating lung function of asthma patients, because asthma is predominantly a disease of airway obstruction. Estimation errors over cystic fibrosis (CF) patients, on the other hand, are higher and the difference could be >5%. The main reason is that CF usually exhibits other symptoms such as infection and mucus accumulation, which affect lung function beyond the changes in airway mechanics. Besides, before hospitalization and treatment, CF patients tend to have markedly lower lung function on force exhaling. All these factors cause highly variant results on the FEV1 error, while FVC reflecting the entire breathing volume is less affected.

9 RELATED WORK

Contactless human sensing: Research efforts have been made to monitor human bodies from remote. Conventional techniques use infrared devices [26] or depth cameras [33] for imaging analysis, and later research achieved accurate sensing with RF signals for fall detection [67], gesture recognition [80] and motion tracking [41]. In particular, these techniques have been adopted for contactless breath monitoring [31, 40, 44, 55, 74, 75]. However, they require extra hardware with high costs and complicated setup, which are unaffordable for daily monitoring out of clinic. In contrast, SpiroSonic uses only the existing hardware of commodity smartphones.

Acoustic motion tracking: Since acoustic signals could be produced by commodity smartphones, they have been widely used to track humans' hand and body motions. Earlier techniques require humans to hand-hold the smartphone and track the smartphone's motion through signal propagation delay [58], Doppler
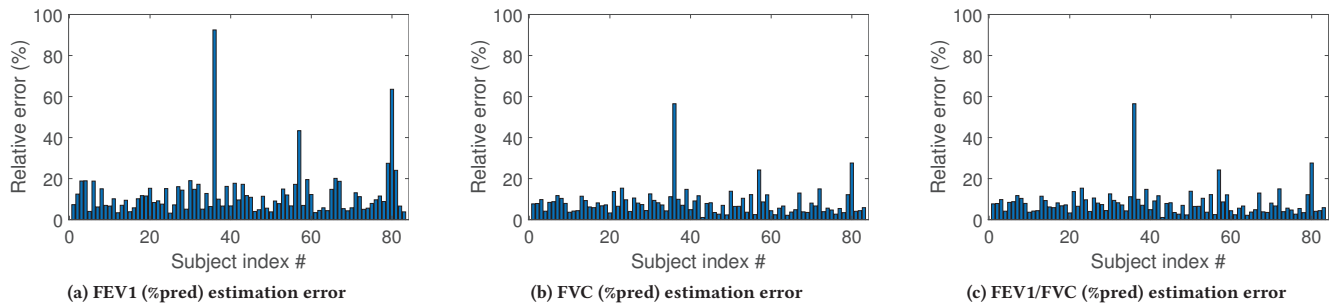
(a) FEV1 (%pred) estimation error

(b) FVC (%pred) estimation error

(c) FEV1/FVC (%pred) estimation error

Figure 27: Errors of estimating lung function for individual patients

(a) Different age subgroups

(b) Different gender subgroups
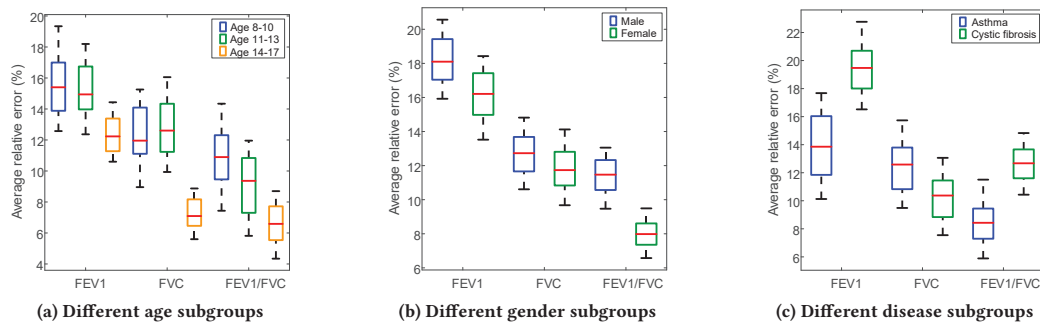
(c) Different disease subgroups

Figure 28: Prediction accuracy over different patient subgroups

shift [3, 32, 76] and frequency difference [45, 71]. Later schemes, instead, focus on device-free motion tracking that analyzes the reflected signal from the target being tracked [53, 66, 73, 77]. These device-free systems, however, require the smartphone to be always stationary. In addition, most systems are limited to tracking the motion of small targets (e.g., human fingers) and their techniques may not be applicable to track the chest wall motion.

Acoustic sensing for mobile healthcare: Acoustic signals have been used for disease diagnosis. For example, ECG sensing was implemented on commodity smartphones [59], and PDVocal [79] diagnoses Parkinson's disease based on abnormal body sounds. These techniques, nevertheless, are orthogonal to the focus of SpiroSonic. Some recent techniques use acoustic signals to measure the humans' respiration rates [15, 27] or breathing events (e.g., apnea) [51, 52, 72] from their breathing motions, and are useful in diagnosing various diseases such as sleep apnea and drug overdose. SpiroSonic further extends these existing work to respiratory disease evaluation, by enabling accurate measurement of lung function indices.

SpiroSonic shares the same design goal with SpiroSmart [39] and SpiroCall [23], which measure lung function indices from humans' audible breathing sounds. However, these systems are sensitive to ambient noise and humans' body motion. SpiroSonic, in contrast, provides better adaptability and reliability in these settings.

10 DISCUSSIONS

Impact of Chest Sizes and Shapes: Being different from existing work that tracks motion of small targets (e.g., human fingers), SpiroSonic tracks the motion of chest wall that has a non-negligible size. Since sound propagates as a pressure wave in air, the ultrasound signal reflected from the chest could be modeled as being transmitted from an imaginary source without extra phase change

[50, 54], if the chest wall is considered as a flat surface. In practice, when it is not ideally flat, SpiroSonic measures the average displacement of different portions of chest wall. The impact of irregular chest shapes, then, is minimized by neural network regression.

Performance over Patients: SpiroSonic has noticeably different measurement accuracies when being applied to healthy humans and patients with pulmonary diseases. The main reason is that our clinical study was conducted over pediatric patients who are less collaborative, resulting in extra errors. Further, since pediatric patients are still in growth, their %pred values may not be well characterized by GLI values [60]. Clinical practices also found that pulmonary diseases result in chest deformity or relevant neuromuscular diseases, which dramatically change the shape of chest. For example, severe chest deformity may lead to big concavity in the chest center [56], which distorts the ultrasound reflection patterns.

11 CONCLUSION

In this paper, we present SpiroSonic, a new mobile system design that precisely monitors humans' lung function from commodity smartphones. SpiroSonic measures the humans' chest wall motion via acoustic sensing, and then converts the measured motion into lung function indices. Clinical studies show that SpiroSonic's measurement error could be as low as 7.7% over pediatric patients.

REFERENCES

[1] EasyOne Air. https://www.nddmed.com/en-us/product/easyone-air.html.
[2] Heba Aly and Moustafa Youssef. 2016. Zephyr: Ubiquitous accurate multi-sensor fusion-based respiratory rate estimation using smartphones. In *IEEE INFOCOM*.
[3] Md Tanvir Islam Aumi, Sidhant Gupta, Mayank Goel, Eric Larson, and Shwetak Patel. 2013. DopLink: using the doppler effect for multi-device interaction. In *Proceedings of the 2013 ACM international joint conference on Pervasive and ubiquitous computing*. 583–586.
[4] Katayoun Bahadori, Mary M Doyle-Waters, Carlo Marra, Larry Lynd, Kadria Alasaly, John Swiston, and Js Mark FitzGerald. 2009. Economic burden of asthma: a systematic review. *BMC pulmonary medicine* 9, 1 (2009), 24.
[5] Andrew Bates, Martin J Ling, Janek Mann, and Damal K Arvind. 2010. Respiratory rate and flow waveform estimation from tri-axial accelerometer data. In *Proceedings of the International Conference on Body Sensor Networks*. 144–150.
[6] Surya P Bhatt, Pallavi P Balte, Joseph E Schwartz, Patricia A Cassano, David Couper, David R Jacobs, Ravi Kalhan, George T O'Connor, Sachin Yende, Jason L Sanders, et al. 2019. Discriminative accuracy of FEV1: FVC thresholds for COPD-related hospitalization and mortality. *Jama* 321, 24 (2019), 2438–2447.
[7] Homer A Boushey, Christine A Sorkness, Tonya S King, Sean D Sullivan, John V Fahy, Stephen C Lazarus, Vernon M Chinchilli, Timothy J Craig, Emily A Dimango, Aaron Deykin, et al. 2005. Daily versus as-needed corticosteroids for mild persistent asthma. *New England Journal of Medicine* 352, 15 (2005), 1519–1528.
[8] PLP Brand and RJ Roorda. 2003. Usefulness of monitoring lung function in asthma. *Archives of disease in childhood* 88, 11 (2003), 1021–1025.
[9] GB Brookes and AJ Fairfax. 1982. Chronic upper airway obstruction: value of the flow volume loop examination in assessment and management. *Journal of the Royal Society of Medicine* 75, 6 (1982), 425.
[10] V Brusasco. 2003. Usefulness of peak expiratory flow measurements: is it just a matter of instrument accuracy? *Thorax* 58, 5 (2003), 375–376.
[11] PMA Calverley. 2009. The clinical usefulness of spirometric information. *Breathe* 5, 3 (2009), 214–220.
[12] William D. Carey. 2010. *Current Clinical Medicine 2nd Edition*. Saunders, Cleveland, OH.
[13] C William Carspecken, Carlos Arteta, and Gari D Clifford. 2013. TeleSpiro: A low-cost mobile spirometer for resource-limited settings. In *Proceedings of the IEEE Point-of-Care Healthcare Technologies (PHT)*. 144–147.
[14] Po-Hsuan Cameron Chen, Yun Liu, and Lily Peng. 2019. How to develop machine learning models for healthcare. *Nature materials* 18, 5 (2019), 410.
[15] Zhenyu Chen, Mu Lin, Fanglin Chen, Nicholas D Lane, Giuseppe Cardone, Rui Wang, Tianxing Li, Yiqiang Chen, Tanzeem Choudhury, and Andrew T Campbell. 2013. Unobtrusive sleep monitoring using smartphones. In *Proceedings of the 7th International Conference on Pervasive Computing Technologies for Healthcare and Workshops*. IEEE, 145–152.
[16] A Czaplinski, AA Yen, and Stanley H Appel. 2006. Forced vital capacity (FVC) as an indicator of survival and disease progression in an ALS clinic population. *Journal of Neurology, Neurosurgery & Psychiatry* 77, 3 (2006), 390–392.
[17] Fernanda de Cordoba Lanza, Anderson Alves de Camargo, Lilian Rocha Ferraz Archija, Jessyca Pachi Rodrigues Selman, Carla Malaguti, and Simone Dal Corso. 2013. Chest wall mobility is related to respiratory muscle strength and lung volumes in healthy subjects. *Respiratory care* 58, 12 (2013), 2107–2112.
[18] Sophie Debouche, Laurent Pitance, Annie Robert, Giuseppe Liistro, and Gregory Reychler. 2016. Reliability and reproducibility of chest wall expansion measurement in young healthy adults. *Journal of manipulative and physiological therapeutics* 39, 6 (2016), 443–449.
[19] Paul Enright, WM Vollmer, B Lamprecht, R Jensen, A Jithoo, W Tan, M Studnicka, P Burney, S Gillespie, and A Sonia Buist. 2011. Quality of spirometry tests performed by 9893 adults in 14 countries: the BOLD Study. *Respiratory medicine* 105, 10 (2011), 1507–1515.
[20] Paul L Enright, Gwen S Skloot, Jean M Cox-Ganser, Iris G Udasin, and Robin Herbert. 2010. Quality of spirometry performed by 13,599 participants in the World Trade Center worker and volunteer medical screening program. *Respiratory Care* 55, 3 (2010), 303–309.
[21] National Center for Environmental Health. 2017. Most Recent National Asthma Data. https://www.cdc.gov/asthma/most_recent_national_asthma_data.htm
[22] JJ Gilmartin and GJ Gibson. 1984. Abnormalities of chest wall motion in patients with chronic airflow obstruction. *Thorax* 39, 4 (1984), 264–271.
[23] Mayank Goel, Elliot Saba, Maia Stiber, Eric Whitmire, Josh Fromm, Eric C Larson, Gaetano Borriello, and Shwetak N Patel. 2016. Spirocall: Measuring lung function over a phone call. In *Proceedings of the 2016 CHI Conference on Human Factors in Computing Systems*. 5675–5685.
[24] Ian Gregg and AJ Nunn. 1973. Peak expiratory flow in normal subjects. *Br Med J* 3, 5874 (1973), 282–284.
[25] Siddharth Gupta, Peter Chang, Nonso Anyigbo, and Ashutosh Sabharwal. 2011. mobileSpiro: accurate mobile spirometry for self-management of asthma. In *Proceedings of the First ACM Workshop on Mobile Systems, Applications, and Services for Healthcare*. 1–6.

[26] Ju Han and Bir Bhanu. 2005. Human activity recognition in thermal infrared imagery. In *2005 IEEE Computer Society Conference on Computer Vision and Pattern Recognition (CVPR'05)-Workshops*. IEEE, 17–17.
[27] Tian Hao, Guoliang Xing, and Gang Zhou. 2013. iSleep: unobtrusive sleep quality monitoring using smartphones. In *Proceedings of the 11th ACM Conference on Embedded Networked Sensor Systems*. 1–14.
[28] Matthew J Hegewald, Heather M Gallo, and Emily L Wilson. 2016. Accuracy and quality of spirometry in primary care offices. *Annals of the American Thoracic Society* 13, 12 (2016), 2119–2124.
[29] Matthew J Hegewald, Michael J Lefor, Robert L Jensen, Robert O Crapo, Stephen B Kritchevsky, Catherine L Haggerty, Douglas C Bauer, Suzanne Satterfield, Tamara Harris, et al. 2007. Peak expiratory flow is not a quality indicator for spirometry: peak expiratory flow variability and FEV1 are poorly correlated in an elderly population. *Chest* 131, 5 (2007), 1494–1499.
[30] M Hibbert, A Lannigan, J Raven, L Landau, and P Phelan. 1995. Gender differences in lung growth. *Pediatric pulmonology* 19, 2 (1995), 129–134.
[31] Chen-Yu Hsu, Aayush Ahuja, Shichao Yue, Rumen Hristov, Zachary Kabelac, and Dina Katabi. 2017. Zero-effort in-home sleep and insomnia monitoring using radio signals. *Proceedings of the ACM on Interactive, Mobile, Wearable and Ubiquitous Technologies* 1, 3 (2017), 1–18.
[32] Wenchao Huang, Yan Xiong, Xiang-Yang Li, Hao Lin, Xufei Mao, Panlong Yang, and Yunhao Liu. 2014. Shake and walk: Acoustic direction finding and fine-grained indoor localization using smartphones. In *IEEE INFOCOM*. 370–378.
[33] Ahmad Jalal, Md Zia Uddin, and T-S Kim. 2012. Depth video-based human activity recognition system using translation and scaling invariant features for life logging at smart home. *IEEE Transactions on Consumer Electronics* 58, 3 (2012), 863–871.
[34] Kerri A Johannson, Eric Vittinghoff, Julie Morisset, Joyce S Lee, John R Balmes, and Harold R Collard. 2017. Home monitoring improves endpoint efficiency in idiopathic pulmonary fibrosis. *European Respiratory Journal* 50, 1 (2017), 1602406.
[35] Hideo Kaneko and Jun Horie. 2012. Breathing movements of the chest and abdominal wall in healthy subjects. *Respiratory care* 57, 9 (2012), 1442–1451.
[36] Hideo Kaneko, Shuichi Shiranita, Jun Horie, and Shinichiro Hayashi. 2016. Reduced chest and abdominal wall mobility and their relationship to Lung function, respiratory muscle strength, and exercise tolerance in subjects with COPD. *Respiratory care* 61, 11 (2016), 1472–1480.
[37] HA Kerstjens, Bert Rijcken, Jan P Schouten, and Dirkje S Postma. 1997. Decline of FEV1 by age and smoking status: facts, figures, and fallacies. *Thorax* 52, 9 (1997), 820.
[38] Peter Lange, Bartolome Celli, Alvar Agustí, Gorm Boje Jensen, Miguel Divo, Rosa Faner, Stefano Guerra, Jacob Louis Marott, Fernando D Martinez, Pablo Martinez-Camblor, et al. 2015. Lung-function trajectories leading to chronic obstructive pulmonary disease. *New England Journal of Medicine* 373, 2 (2015), 111–122.
[39] Eric C Larson, Mayank Goel, Gaetano Boriello, Sonya Heltshe, Margaret Rosenfeld, and Shwetak N Patel. 2012. SpiroSmart: using a microphone to measure lung function on a mobile phone. In *Proceedings of the ACM Conference on ubiquitous computing*. 280–289.
[40] Gregory F Lewis, Rodolfo G Gatto, and Stephen W Porges. 2011. A novel method for extracting respiration rate and relative tidal volume from infrared thermography. *Psychophysiology* 48, 7 (2011), 877–887.
[41] Tianhong Li, Lijie Fan, Mingmin Zhao, Yingcheng Liu, and Dina Katabi. 2019. Making the invisible visible: Action recognition through walls and occlusions. In *Proceedings of the IEEE International Conference on Computer Vision*. 872–881.
[42] Giuseppe Liistro, Carl Vanwelde, Walter Vincken, Jan Vandevoorde, Geert Verleden, Johan Buffels, et al. 2006. Technical and functional assessment of 10 office spirometers. *Chest* 130, 3 (2006), 657–665.
[43] Guan-Zheng Liu, Yan-Wei Guo, Qing-Song Zhu, Bang-Yu Huang, and Lei Wang. 2011. Estimation of respiration rate from three-dimensional acceleration data based on body sensor network. *Telemedicine and e-health* 17, 9 (2011), 705–711.
[44] Jian Liu, Yan Wang, Yingying Chen, Jie Yang, Xu Chen, and Jerry Cheng. 2015. Tracking vital signs during sleep leveraging off-the-shelf wifi. In *Proceedings of the 16th ACM International Symposium on Mobile Ad Hoc Networking and Computing*. 267–276.
[45] Wenguang Mao, Jian He, and Lili Qiu. 2016. CAT: high-precision acoustic motion tracking. In *Proceedings of the 22nd Annual International Conference on Mobile Computing and Networking*. 69–81.
[46] Sameer K Mathur and William W Busse. 2006. Asthma: diagnosis and management. *Medical Clinics* 90, 1 (2006), 39–60.
[47] Michael J McGeachie, Katherine P Yates, Xiaobo Zhou, Feng Guo, Alice L Sternberg, Mark L Van Natta, Robert A Wise, Stanley J Szefler, Sunita Sharma, Alvin T Kho, et al. 2016. Patterns of growth and decline in lung function in persistent childhood asthma. *New England Journal of Medicine* 374, 19 (2016), 1842–1852.
[48] MicroLife. PF 100 Asthma monitor. https://www.microlife.com/consumer-products/respiratory-care/asthma-monitor/pf-100
[49] Martin R Miller, JATS Hankinson, V Brusasco, F Burgos, R Casaburi, A Coates, R Crapo, P vd Enright, CPM Van der Grinten, P Gustafsson, et al. 2005. Standardisation of spirometry. *European respiratory journal* 26, 2 (2005), 319–338.

Xingzhe Song, Boyuan Yang, Ge Yang, Ruirong Chen, Erick Forno, Wei Chen and Wei Gao

[50] John Edwin Moore. 1979. *Design for good acoustics and noise control.* Macmillan International Higher Education.

[51] Rajalakshmi Nandakumar, Shyamnath Gollakota, and Jacob E Sunshine. 2019. Opioid overdose detection using smartphones. *Science translational medicine* 11, 474 (2019).

[52] Rajalakshmi Nandakumar, Shyamnath Gollakota, and Nathaniel Watson. 2015. Contactless sleep apnea detection on smartphones. In *Proceedings of the 13th annual international conference on mobile systems, applications, and services.* 45–57.

[53] Rajalakshmi Nandakumar, Vikram Iyer, Desney Tan, and Shyamnath Gollakota. 2016. Fingerio: Using active sonar for fine-grained finger tracking. In *Proceedings of the 2016 CHI Conference on Human Factors in Computing Systems.* 1515–1525.

[54] Rod Nave. 2000. *HyperPhysics.* Georgia State University, Department of Physics and Astronomy.

[55] Phuc Nguyen, Xinyu Zhang, Ann Halbower, and Tam Vu. 2016. Continuous and fine-grained breathing volume monitoring from afar using wireless signals. In *IEEE INFOCOM.*

[56] Robert J Obermeyer and Michael J Goretsky. 2012. Chest wall deformities in pediatric surgery. *Surgical Clinics* 92, 3 (2012), 669–684.

[57] Hayrettin Okut. 2016. Bayesian regularized neural networks for small n big p data. *Artificial neural networks-models and applications* (2016).

[58] Chunyi Peng, Guobin Shen, Yongguang Zhang, Yanlin Li, and Kun Tan. 2007. Beepbeep: a high accuracy acoustic ranging system using cots mobile devices. In *Proceedings of the 5th international conference on Embedded networked sensor systems.* 1–14.

[59] Kun Qian, Chenshu Wu, Fu Xiao, Yue Zheng, Yi Zhang, Zheng Yang, and Yunhao Liu. 2018. Acousticcardiogram: Monitoring heartbeats using acoustic signals on smart devices. In *IEEE INFOCOM.* 1574–1582.

[60] Philip H Quanjer, Sanja Stanojevic, Tim J Cole, Xaver Baur, Graham L Hall, Bruce H Culver, Paul L Enright, John L Hankinson, Mary SM Ip, and Jinping Zheng. 2012. Multi-ethnic reference values for spirometry for the 3–95-yr age range: the global lung function 2012 equations. *European Respiratory Journal* 40, 6 (2012), 1324–1343.

[61] Mohammad Reza Raoufy, Sohrab Hajizadeh, Shahriar Gharibzadeh, Ali R Mani, Parivash Eftekhari, and Mohammad Reza Masjedi. 2013. Nonlinear model for estimating respiratory volume based on thoracoabdominal breathing movements. *Respirology* 18, 1 (2013), 108–116.

[62] Helen Reddel, Sandra Ware, Guy Marks, Cheryl Salome, Christine Jenkins, and Ann Woolcock. 1999. Differences between asthma exacerbations and poor asthma control. *The Lancet* 353, 9150 (1999), 364–369.

[63] Ravi S Reddy, Khalid A Alahmari, Paul S Silvian, Irshad A Ahmad, Venkata Nagaraj Kakarparthi, and Kanagaraj Rengaramanujam. 2019. Reliability of chest wall mobility and its correlation with lung functions in healthy nonsmokers, healthy smokers, and patients with COPD. *Canadian respiratory journal* 2019 (2019).

[64] Medical International Research. MIR Smart ONE. https://www.mirsmartone.com/?page_id=1587&lang=en

[65] Bersain A Reyes, Natasa Reljin, Youngsun Kong, Yunyoung Nam, and Ki H Chon. 2016. Tidal volume and instantaneous respiration rate estimation using a volumetric surrogate signal acquired via a smartphone camera. *IEEE journal of biomedical and health informatics* 21, 3 (2016), 764–777.

[66] Ke Sun, Ting Zhao, Wei Wang, and Lei Xie. 2018. Vskin: Sensing touch gestures on surfaces of mobile devices using acoustic signals. In *Proceedings of the 24th Annual International Conference on Mobile Computing and Networking.* 591–605.

[67] Yonglong Tian, Guang-He Lee, Hao He, Chen-Yu Hsu, and Dina Katabi. 2018. RF-based fall monitoring using convolutional neural networks. *Proceedings of the ACM on Interactive, Mobile, Wearable and Ubiquitous Technologies* 2, 3 (2018), 1–24.

[68] Jonathan L Ticknor. 2013. A Bayesian regularized artificial neural network for stock market forecasting. *Expert Systems with Applications* 40, 14 (2013), 5501–5506.

[69] Mary C Townsend, Occupational, Environmental Lung Disorders Committee, et al. 2011. Spirometry in the occupational health setting–2011 update. *Journal of occupational and environmental medicine* 53, 5 (2011), 569.

[70] Yu-Chih Tung, Duc Bui, and Kang G Shin. 2018. Cross-platform support for rapid development of mobile acoustic sensing applications. In *Proceedings of the 16th Annual International Conference on Mobile Systems, Applications, and Services.* 455–467.

[71] Anran Wang and Shyamnath Gollakota. 2019. Millisonic: Pushing the limits of acoustic motion tracking. In *Proceedings of the 2019 CHI Conference on Human Factors in Computing Systems.* 1–11.

[72] Anran Wang, Jacob E Sunshine, and Shyamnath Gollakota. 2019. Contactless infant monitoring using white noise. In *The 25th Annual International Conference on Mobile Computing and Networking.* 1–16.

[73] Wei Wang, Alex X Liu, and Ke Sun. 2016. Device-free gesture tracking using acoustic signals. In *Proceedings of the 22nd Annual International Conference on Mobile Computing and Networking.* 82–94.

[74] Meng-Chieh Yu, Jia-Ling Liou, Shuenn-Wen Kuo, Ming-Sui Lee, and Yi-Ping Hung. 2012. Noncontact respiratory measurement of volume change using depth camera. In *Proceedings of the Annual International Conference of the IEEE Engineering in Medicine and Biology Society.* 2371–2374.

[75] Shichao Yue, Hao He, Hao Wang, Hariharan Rahul, and Dina Katabi. 2018. Extracting multi-person respiration from entangled RF signals. *Proceedings of the ACM on Interactive, Mobile, Wearable and Ubiquitous Technologies* 2, 2 (2018), 1–22.

[76] Sangki Yun, Yi-Chao Chen, and Lili Qiu. 2015. Turning a mobile device into a mouse in the air. In *Proceedings of the 13th Annual International Conference on Mobile Systems, Applications, and Services.* 15–29.

[77] Sangki Yun, Yi-Chao Chen, Huihuang Zheng, Lili Qiu, and Wenguang Mao. 2017. Strata: Fine-grained acoustic-based device-free tracking. In *Proceedings of the 15th annual international conference on mobile systems, applications, and services.* 15–28.

[78] A Zapletal and J Chalupova. 2003. Forced expiratory parameters in healthy preschool children (3–6 years of age). *Pediatric pulmonology* 35, 3 (2003), 200–207.

[79] Hanbin Zhang, Chen Song, Aosen Wang, Chenhan Xu, Dongmei Li, and Wenyao Xu. 2019. PDVocal: Towards Privacy-preserving Parkinson's Disease Detection using Non-speech Body Sounds. In *The 25th Annual International Conference on Mobile Computing and Networking.* 1–16.

[80] Jie Zhang, Zhanyong Tang, Meng Li, Dingyi Fang, Petteri Nurmi, and Zheng Wang. 2018. CrossSense: Towards cross-site and large-scale WiFi sensing. In *Proceedings of the 24th Annual International Conference on Mobile Computing and Networking.* 305–320.